A NEW LOOK ON THE PLASTIC BUCKLING PARADOX

Zvi Zuckerman*
Faculty of Aerospace Engineering
Technion - Israel Institute of Technology
Haifa 32000, Israel

Abstract

This paper examines the elastoplastic buckling of a rectangular plate, with different boundary conditions, under uniform compression combined with uniform tension in the perpendicular direction. The analysis is based on the standard linear buckling equations and material behaviour is modelled by the small strain J_2 flow and deformation theories of plasticity. For sufficiently thin plates we recover with both theories the classical elastic results. However, for thicker plates there is a remarkable difference in the buckling loads predicted by these two theories. Apart from the expected observation that deformation theory gives lower critical stresses than those obtained from the flow theory, we have discovered the existence of an **optimal loading path** for the deformation theory model. Buckling loads attained along that optimal path - specified by particular compression/tension ratios -- are the highest possible over the entire space of loading histories. By contrast, no similar optimum has been found with the flow theory. This striking contradiction in the buckling behaviour, obtained from the two competing plastic theories, sheds new light on the plastic buckling paradox. The paper contains also a detailed parametric study over a range of plate geometries and for different material properties. The results are of considerable interest for the aerospace industry since biaxial stress fields are rather common in thin walled structures.

1. Background

Plastic buckling phenomena have provided during the last four decades some of the crucial test cases in regard to the validity of metal plasticity theories. Indeed, the difference in the critical load predictions obtained from the flow theory and deformation theories became known as the plastic buckling paradox. In a recent study [1], on the elastoplastic buckling of annular plates in pure shear, it has been found that flow theory predictions may exceed those of deformation theory by a factor of 17. Experimental data in that case is in agreement with the deformation theory predictions. Of course, there are cases where the critical stresses obtained from the two theories are nearly equal. A typical example is furnished by axially-symmetric buckling of axially compressed circular cylindrical shells. For materials with a relatively high power law exponent there is little difference in the buckling stresses predicted by the two theories[2]. There is, however, a general agreement among engineers and researchers that (a) deformation theory is less physically correct than flow theory, but (b) deformation theory predicts buckling loads that are smaller than those obtained with flow theory, and (c) experimental evidence points in favour of deformation theory results.

Most existing studies, however, are concerned with a single load parameter, like the problems in papers[1],[2]. An early exception to this appears to be a 1968 NASA report[3] on plastic buckling of plates and shells under biaxial loading.

The present paper examines in detail the elastoplastic buckling of a rectangular plate under biaxial loads. The study follows a recent paper[4] on the same problem though of more restricted nature in as much no flow theory results were discussed. Here we present a full account of buckling data obtained with both theories and over a range of plate geometries and for different material properties. Solutions are derived with different boundary conditions (simply supported or clamped edges) via a separation of variables solution method.

The main finding of the study is the existence of an optimal loading path for the deformation theory model. Buckling loads attained along that loading path -- specified by particular compression/tension ratios -- are the highest possible over the entire space of loading histories. By contrast, no similar optimum has been found with the flow theory. This striking contradiction in the buckling behaviour, obtained from the two competing plastic theories, sheds new light on the plastic buckling paradox. It is hoped that the theoretical data that emerges from this study will be put to an appropriate laboratory test which will support its validity.

2. Governing Equations

A rectangular plate of length a, width b, and uniform thickness h (see Fig. 1) is subjected to axial compression $\sigma_y=-P$ along with axial tension $\sigma_x=\xi P$ where ξ is a fixed parameter. Thus, with $\xi=0$ we have simple axial compression, while $\xi=-1$ describes equibiaxial compression.

With $\dot{w}$ denoting the out of plane velocity during buckling we have the plate buckling equation

$$\frac{h^2}{12}\left[E_{xx}\dot{w}_{,xxxx} + 2(E_{xx} + 2G_{xy})\dot{w}_{,xxyy} + E_{yy}\dot{w}_{,yyyy}\right] - \xi P\dot{w}_{,xx} + P\dot{w}_{,yy} = 0 \qquad (1)$$

*This paper is based on a part of a thesis submitted to the Technion, in partial fulfillment of the requirements for the degree of Master of Science.

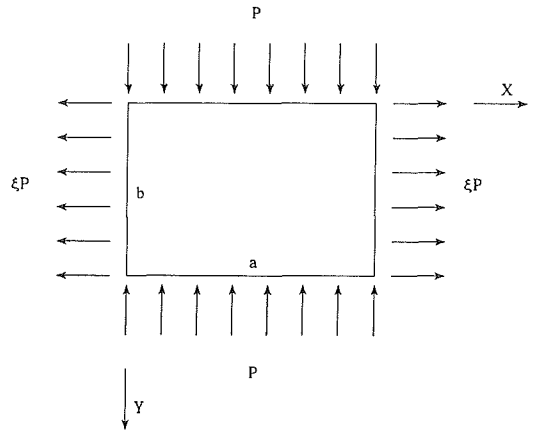

Figure 1 - Notation for Rectangular Plate.

where $(E_{xx}, E_{xy}, E_{yy}, G_{xy})$ are the instantaneous moduli of the plane-stress constitutive relations

$$\dot{\sigma}_x = E_{xx}\dot{\varepsilon}_x + E_{xy}\dot{\varepsilon}_y \tag{2a}$$

$$\dot{\sigma}_y = E_{xy}\dot{\varepsilon}_x + E_{yy}\dot{\varepsilon}_y \tag{2b}$$

$$\dot{\tau}_{xy} = 2G\dot{\gamma}_{xy} \tag{2c}$$

Here $(\dot{\sigma}_x, \dot{\sigma}_y, \dot{\tau}_{zy})$ are the stress rate components, while $(\dot{\varepsilon}_x, \dot{\varepsilon}_y, \dot{\gamma}_{xy})$ are the strain rate components.

Equation (1) is supplemented by eight boundary conditions - two on each side of the plate. Taking the boundaries x=0,a as an example, we have for simple supports

$$\dot{w} = 0 \qquad \dot{w}_{,xx} = 0 \tag{3a}$$

while for clamped edges

$$\dot{w} = 0 \qquad \dot{w}_{,x} = 0 \tag{3b}$$

Similar conditions are imposed along the perpendicular boundaries y=0, b.

The instantaneous moduli that appear in Eq. (1) depend on the plasticity theory used to model material behaviour. For the J_2 flow theory we have, with the usual notation,

$$\dot{\sigma}_{ij} = 2G\dot{\varepsilon}_{ij} + \lambda\delta_{ij}\dot{\varepsilon}_{kk} - 3(G - G_T)\frac{S_{ij}S_{kl}\dot{\varepsilon}_{kl}}{\sigma_e^2} \tag{4}$$

where $\dot{\sigma}_{ij}$ are the stress rate components, $\dot{\varepsilon}_{ij}$ - the strain rate components, (G,λ) - the elastic constants, S_{ij} - the stress deviator components, σ_e is the effective stress, and G_T is the tangent shear modulus defined by

$$\frac{1}{G_T} = \frac{1}{G} + 3\left(\frac{1}{E_T} - \frac{1}{E}\right) \tag{5}$$

where E_T is the tangent modulus obtained from the uniaxial stress-strain curve.

Similarly, the rate form of the J_2 deformation theory reads

$$\dot{\sigma}_{ij} = 2G_s\dot{\varepsilon}_{ij} + \lambda_s\delta_{ij}\dot{\varepsilon}_{kk} - 3(G_s - G_T)\frac{S_{ij}S_{kl}\dot{\varepsilon}_{kl}}{\sigma_e^2} \tag{6}$$

where (G_s, λ_s) are the secant moduli defined by

$$G_s = \frac{E_s}{2(1+\nu_s)} \qquad \lambda_s = \frac{\nu_s E_s}{(1+\nu_s)(1-2\nu_s)} \tag{7}$$

ν_s being the secant Poisson ratio (E, ν are the usual elastic constants)

$$\nu_s = \frac{1}{2} - \left(\frac{1}{2} - \nu\right)\frac{E_s}{E} \tag{8}$$

and E_s is the secant modulus obtained from the uniaxial stress-strain curve.

Specifying (4) and (6) for the present problem, with $\sigma_1=\sigma_x$, $\sigma_2=\sigma_y$ and $\sigma_3=\sigma_z=0$, it is convenient to redefine the instantaneous moduli as

$$\mu_{11} = E_{xx} \qquad \mu_{22} = E_{yy} \qquad \mu_{12} = E_{xy} + 2G_{xy} \tag{9}$$

Thus, with the flow theory we get[4]

$$\mu_{ij} = \frac{4G(G+\lambda) - (G-G_T)[(2G+3\lambda)\Sigma_i\Sigma_j - G(\Sigma_i-\Sigma_j)^2 + \frac{4}{3}G]}{2G + \lambda - \frac{1}{3}(G-G_T)(\Sigma_1+\Sigma_2)^2} \qquad i,j = 1,2 \tag{10}$$

while for the deformation theory we find

$$\mu_{ij} = \frac{4G_s(G_s+\lambda_s) - (G_s-G_T)[(2G_s+3\lambda_s)\Sigma_i\Sigma_j - G_s(\Sigma_i-\Sigma_j)^2 + \frac{4}{3}G_s]}{2G_s + \lambda_s - \frac{1}{3}(G_s-G_T)(\Sigma_1+\Sigma_2)^2} \qquad i,j = 1,2 \tag{11}$$

The effective stress is now given by

$$\sigma_e^2 = (1 + \xi + \xi^2)P^2 \tag{12}$$

and the normalized prebuckling stresses, $\Sigma_i = \sigma_i/\sigma_e$ i=1,2, are

$$\Sigma_1 = \frac{\xi}{\sqrt{1+\xi+\xi^2}} \qquad \Sigma_2 = -\frac{\xi}{\sqrt{1+\xi+\xi^2}} \tag{13}$$

To sum up, for given plate geometry, boundary conditions, material properties (μ_{ij}) and loading program (ξ), we seek the smallest value of P for which Eq. (1) admits a nontrivial solution. That eigenvalue is identified with the critical load which causes buckling of the plate. Any uniaxial stress strain relation can be implemented in this analysis. The examples presented later were calculated with the Ramberg Osgood elastoplastic formula

$$\varepsilon = \frac{\sigma_e}{E} + K\left(\frac{\sigma_e}{E}\right)^n \tag{14}$$

where (K,n) are material parameters.

3. Separation of Variables Solution

The simplest solution of (1) is obtained for simply supported boundaries, namely $\dot{w}=\dot{w}_{,xx}=0$ at $x=0,a$, and $\dot{w}=\dot{w}_{,yy}=0$ at $y=0,b$. These constraints are met with the velocity field

$$\dot{w} = A\sin\left(\frac{m\pi x}{a}\right)\sin\left(\frac{n\pi y}{b}\right) \qquad m,n = 1,2,\ldots \qquad (15)$$

where, A is an arbitrary constant. Inserting (15) in (1) we get the eigenvalue equations[4]

$$\left[2G + \lambda - \frac{1}{3}(G-G_T)(\Sigma_1+\Sigma_2)^2\right](\xi m^2-\beta^2n^2)P$$

$$+ \alpha\left\{\frac{4}{3}G(2G+3\lambda+G_T)(m^2+\beta^2n^2)^2 -\right.$$

$$(G-G_T)[(2G+3\lambda)(m^2\Sigma_1+\beta^2n^2\Sigma_2)^2$$

$$\left. - 2\beta^2m^2n^2G(\Sigma_1-\Sigma_2)^2]\right\} = 0 \qquad (16)$$

for the flow theory, and

$$\left[2G_s + \lambda_s - \frac{1}{3}(G_s-G_T)(\Sigma_1+\Sigma_2)^2\right](\xi m^2-\beta^2n^2)P$$

$$+ \alpha\left\{\frac{4}{3}G_s(2G_s+3\lambda_s+G_T)(m^2+\beta^2n^2)^2 -\right.$$

$$(G_s-G_T)[(2G_s+3\lambda_s)(m^2\Sigma_1+\beta^2n^2\Sigma_2)^2$$

$$\left. - 2\beta^2m^2n^2G_s(\Sigma_1-\Sigma_2)^2]\right\} = 0 \qquad (17)$$

for the deformation theory. The geometrical parameters (α,β) are defined by

$$\alpha = \frac{\pi^2h^2}{12a^2} \qquad \beta = \frac{a}{b} \qquad (18)$$

when $G_T=G_s=G$ and $\lambda_s=\lambda$ we recover from both (16) and (17) the linear elastic buckling equation[5]

$$\frac{(1-\nu^2)P}{\alpha E} = \frac{\beta^2n^2+m^2}{\beta^2n^2-\xi m^2} \qquad (19)$$

Accordingly, we shall refer to the nondimensional buckling parameter (not to be confused with the Ramberg Osgood constant in (14))

$$K = \frac{(1-\nu^2)P}{\alpha E} \qquad (20)$$

as a suitable measure of the critical loads. Notice that the smallest eigenvalues of (16)-(17) should be minimized with respect to the wave numbers (m,n).

We turn now to the case where the boundaries $x=0,a$ are simply supported (3a), but the compressed sides are clamped. It is convenient here to locate the origin of the (x,y) axes at the center of the boundary $x=0$ (see Fig. 2) so that the clamped boundary conditions read

$$\dot{w} = 0 \qquad \dot{w}_{,y} = 0 \qquad \text{at} \qquad y = \pm\frac{b}{2} \qquad (21)$$

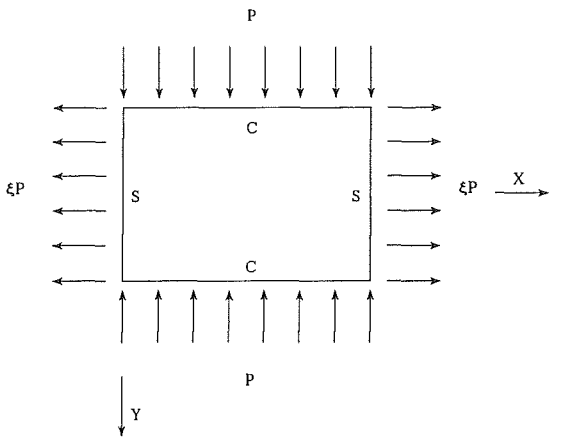

Figure 2 - Rectangular Plate. s - simple support. c - clamped boundary.

The buckling mode is now written in the form

$$\dot{w} = A\sin\left(\frac{m\pi x}{a}\right)f(y) \qquad m = 1,2,\ldots \qquad (22)$$

where $f(y)$ is to be determined. The field (22) complies with the boundary data (3a), and when substituted in (1) results in the ordinary differential equation

$$\frac{h^2}{12}\left[\mu_{11}\left(\frac{\pi m}{a}\right)^4 f - 2\mu_{12}\left(\frac{\pi m}{a}\right)^2 f'' + \mu_2 f''''\right]$$

$$+ \xi P\left(\frac{m\pi}{a}\right)^2 f + Pf'' = 0 \quad , \quad (\cdot)' = \frac{d(\cdot)}{dy} \qquad (23)$$

The solution of this equation has a symmetric part

$$f_1(y) = D_2\sinh\left(\pi\gamma_1\frac{y}{a}\right) + D_4\sinh\left(\pi\gamma_3\frac{y}{a}\right) \qquad (24)$$

and an antisymmetric part

$$f_2(y) = D_1\cosh\left(\pi\gamma_1\frac{y}{a}\right) + D_2\cosh\left(\pi\gamma_3\frac{y}{a}\right) \qquad (25)$$

where $D_i(i=1,\ldots,4)$ are integration constants and (γ_1,γ_3) are the characteristics roots of (23) as determined from the equation

$$\alpha\mu_{22}\gamma^4 + (P-2\mu_{12}\alpha m^2)\gamma^2 + \alpha\mu_{11}m^4 + \xi Pm^2 = 0 \qquad (26)$$

$$m = 1,2,\ldots$$

This equation has four roots labelled as $\pm\gamma_1$ and $\pm\gamma_3$. We skip here much of the algebra involved in the analysis, and for more details one should consult the original thesis[6], or the forthcoming report[7].

The standard technique of compliance with boundary conditions (21) and the requirement for a non trivial solution[6]-[7] leads to the eigenvalue equations. For symmetric buckling modes (24) we get

$$\gamma_3 \tanh\left(\frac{\pi}{2\beta}\gamma_3\right) - \gamma_1 \tanh\left(\frac{\pi}{2\beta}\gamma_1\right) = 0 \qquad (27)$$

while for antisymmetric modes (25) we have

$$\gamma_3 \tanh\left(\frac{\pi}{2\beta}\gamma_1\right) - \gamma_1 \tanh\left(\frac{\pi}{2\beta}\gamma_3\right) = 0 \qquad (28)$$

The solution of (27)-(28) provides the critical buckling parameter (20). Both modes have to be considered in the calculations along with a minimization procedure with respect to the wave number m.

Proceeding along similar lines we can solve the problem when the compressed sides are simply supported and the other edges clamped. here we move the origin of the coordinates to the center of the side y=0, so that at y=0,b, $\dot{w}=\dot{w}_{,yy}=0$ while at $x=\pm\frac{a}{2}$, $\dot{w}=\dot{w}_{,x}=0$. A solution is now sought in the form

$$\dot{w} = Ag(x)\sin\left(\frac{n\pi y}{b}\right) \qquad n = 1,2,\ldots \qquad (29)$$

and the eigenvalue equations follow as

$$\gamma_3 \tanh\left(\frac{\pi}{2}\beta\gamma_3\right) - \gamma_1 \tanh\left(\frac{\pi}{2}\beta\gamma_1\right) = 0 \qquad (30)$$

for symmetric modes, and

$$\gamma_3 \tanh\left(\frac{\pi}{2}\beta\gamma_1\right) - \gamma_1 \tanh\left(\frac{\pi}{2}\beta\gamma_3\right) = 0 \qquad (31)$$

for antisymmetric modes.

The characteristic roots $\pm\gamma_1$ and $\pm\gamma_3$ are determined by the transcendental equation

$$\alpha\beta^2\mu_{11}\gamma^4 - (\xi P + 2\mu_{12}\alpha\beta^2 n^2)\gamma^2 + 2\beta^2\mu_{22}n^4 - Pn^2 = 0$$

$$n = 1,2,\ldots \qquad (32)$$

Solution procedure parallel that of the previous problem including minimization with respect to wave numbers n.

4. Numerical Examples and Discussion

Critical stresses were evaluated numerically by solving the eigenvalue equations (16)-(17), (27)-(28) and (30)-(31) for the different boundary conditions. The solution is straightforward though care has to be exercised in handling the complex roots of (26) and (32). As we have said already, the numerical routine includes a searching technique to trace the smallest eigenvalue (20).

Results for aluminum Al 7075-T6 are shown in Fig. 3 for simply supported plates with $\alpha=0.001$ and $\beta=1$. The Ramberg-Osgood parameters (14) for that metal are $K=3.94\cdot10^{21}$, n=10.9, and the elastic constants are given by $E=7.24\cdot10^{10}$ Pa, $\nu=0.32$.

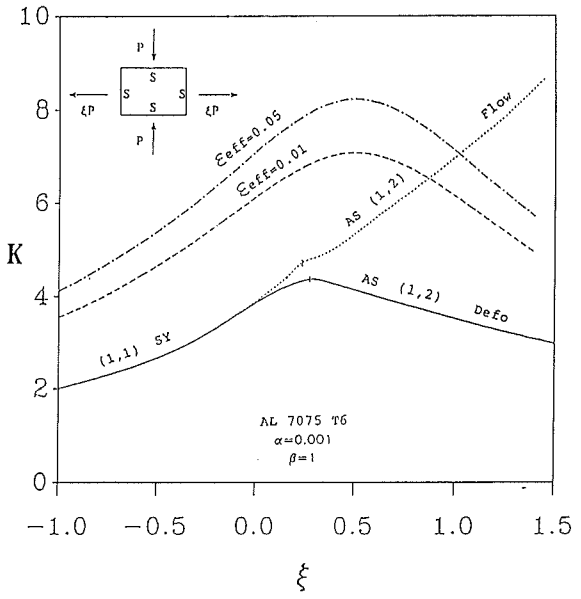

Figure 3 - Variation of Buckling Parameter with Load Ratio.

Initially, for low values of ξ both theories are in agreement, but with increasing load ratio flow theory predicts increasingly higher values of K as compared to the deformation theory. Furthermore, the deformation theory predicts an optimal buckling load at a specific value of ξ. That behaviour is more emphasized in Figs. 4-5 which display the gradual transition from the elastic range (with $\alpha=0.0001$) to the deep plastic range ($\alpha=0.002$) by increasing the plate's thickness.

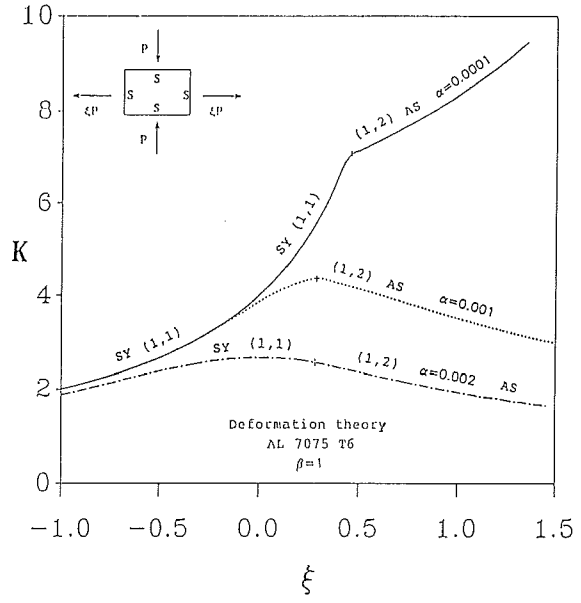

Figure 4 - Influence of Plate Thickness. Deformation Theory.

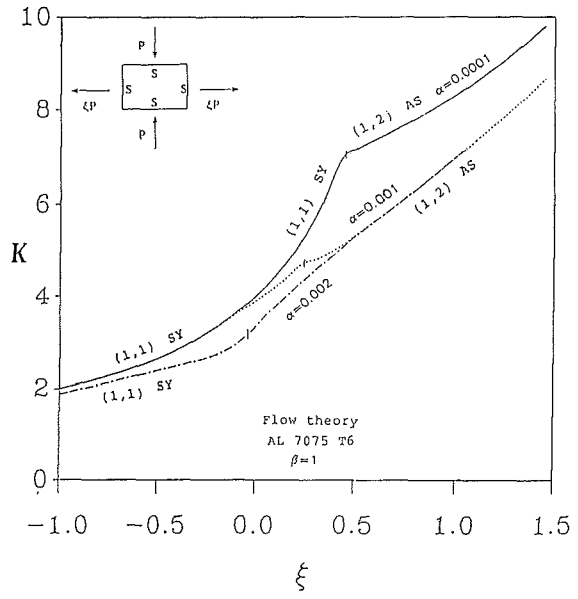

Figure 5 - Influence of Plate Thickness. Flow Theory.

When the plate is more narrow (increasing β) optimal buckling is attained by biaxial compression (see Fig. 6). It is interesting therefore that there exists a critical value of plate aspect ration (β) for which the highest buckling load is obtained in purely uniaxial compression (ξ=0). This observation can be helpful in optimal design of stiffness spacing.

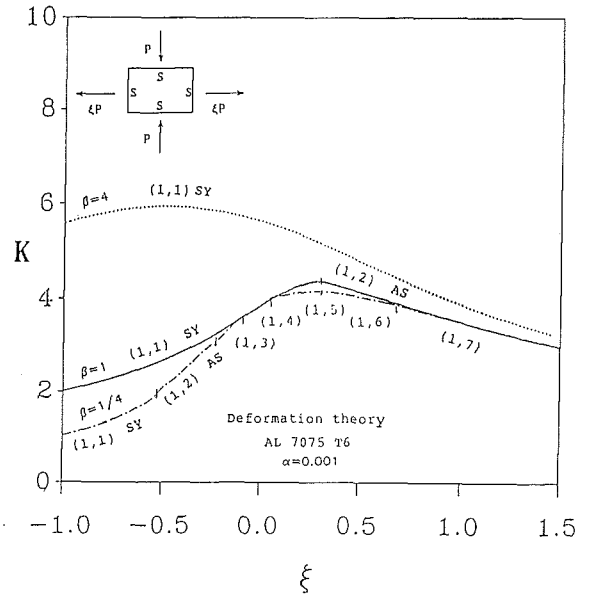

Figure 6 - Influence of Plate Dimensions. Deformation Theory.

Results for the other boundary conditions reveal a similar picture. Of course, clamped plates buckle at higher loads in comparison with simply supported plates, but the contrast between flow and deformation theories remains very much the same (see Figs. 7 and 8).

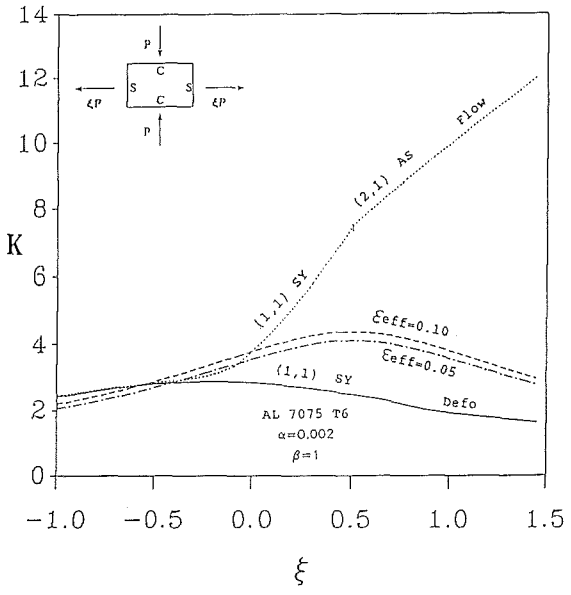

Figure 7 - Buckling with Two Clamped Boundaries.

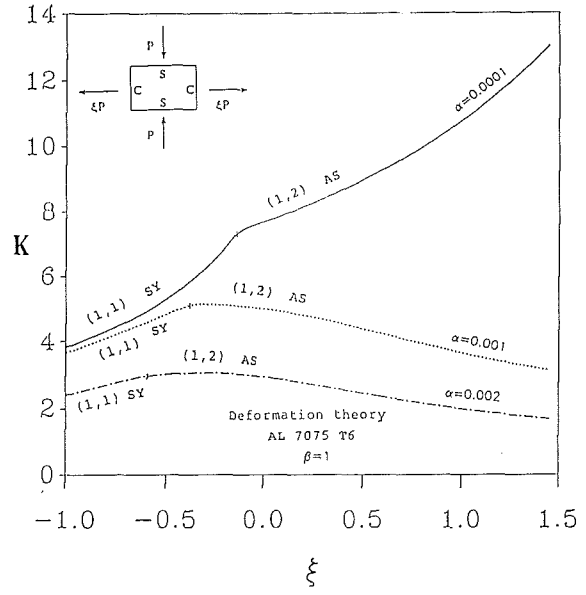

Figure 8 - Influence of Plate Thickness. Deformation Theory. Two Boundaries are Clamped.

References

1. Ore, E. and Durban, D., "Elastoplastic buckling of annular plates is pure shear", *J. Appl. Mech.*, 56, 1989, pp. 644-651.

2. Ore, E. and Durban, D., "Elastoplastic buckling of axially compressed circular cylindrical shells", 1992, submitted for publication.

3. Peterson, J.P., "Plastic buckling of plates and shells under biaxial loading", NASA TN D-4706, 1968.

4. Durban, D., "Plastic buckling of rectangular plates under biaxial loading", in *Buckling of Structures*, Elsevier, 1988, pp. 183-194.

5. Timoshenko, S.P. and Gere, J.M., "*Theory of Elastic Stability*", 2nd edition, McGraw Hill, 1960.

6. Zuckerman, Z., "Optimal path in elastoplastic buckling of plates", M.Sc. Research Thesis, Technion, Haifa, 1992.

7. Durban, D. and Zuckerman, Z., "Optimal buckling of elastoplastic plates under biaxial loading", in preparation.